

Effects of Subsurface Boron and Phosphorus on Surface Reactivity of Si(001): Water and Ammonia Adsorption

Yun Wang, Soo-Hwan Lee, and Gyeong S. Hwang*

Department of Chemical Engineering and Institute of Theoretical Chemistry, The University of Texas at Austin, Austin, Texas 78712

Received: October 27, 2003; In Final Form: July 6, 2004

Using density functional slab calculations with planewave basis set and pseudopotentials, we have examined the effect of subsurface boron and phosphorus on the surface chemical properties of Si(001). We compare the adsorption behaviors of water and ammonia between B- or P-modified and clean Si(001) surfaces. On the B-modified surface, the charge polarization of two B-connected dimers is altered significantly. Our calculation shows that approximately one electron is transferred from the local surface to the subsurface boron, thereby leading both buckled-up and -down atoms of B-connected dimers to be electron-poor (electrophilic). On the other hand, subsurface P brings about no significant change in surface electronic structure. Only about one-tenth of an electron is transferred from the subsurface P to the local surface. As a result, relative to the clean surface, the adsorption properties of water and ammonia change noticeably on the B-modified surface while varying insignificantly on the P-modified surface.

1. Introduction

Atomic-level manipulation of surface chemical properties becomes essential for the fabrication of ever smaller semiconductor devices as well as a range of future molecular devices.^{1–3} The electronic structure of semiconductor surfaces can be modified by surface reconstruction, defects, impurities, and adsorbates, which will in turn alter physical and chemical processes occurring on the surfaces. Because of such complex structural and chemical effects, dynamics at semiconductor surfaces have not been fully understood.

Chemical doping has been widely employed to engineer the electrical properties of semiconductors. By virtue of its well-established process technology, recently, great attention has been drawn to the use of dopant impurities in modifying surface properties. For instance, group V impurities, like arsenic, antimony, and bismuth, have been widely employed as surfactants to control surface stress in heteroepitaxial growth.⁴ In addition, for formation of ultrashallow junction with high dopant concentrations (required for nanometer-scale electronic devices), in situ chemical doping has been recognized as a working alternative to currently widely used low-energy ion implantation.⁵ To achieve precise control of doping profiles, it would be necessary to better understand the effect of surface and/or subsurface dopant atoms on surface chemical reactions, along with the effect of adsorbates on dopant dynamics at the surface and/or subsurface layers. As device dimensions shrink below 100 nm, indeed, the dopant–surface interactions become of great concern in various device manufacturing processes, such as etching and deposition.^{6,7}

In addition, one could envisage atomic-scale manipulation of surface chemical properties by incorporating dopant atoms into the surface or subsurface.⁸ A detailed understanding of the potential role of dopants as possible reaction promoters or inhibitors will contribute significantly to finding a new and

reliable way to construct desired organic function assembly on a semiconductor surface for various chemical, biological, and electronic applications.

In this paper, we present the function of subsurface B and P on water and ammonia adsorption on Si(001)-2 × 1 using density functional theory (DFT) slab calculations. The primary objective of this work is to provide a physical picture of atomic-scale manipulation of surface reactivity using dopant impurities as reaction promoters or inhibitors.

Boron and phosphorus are the most widely used p-type and n-type impurities in Si, respectively. It is well-known that B prefers to remain at the subsurface,⁹ but P appears to exist preferably on the surface (rather than at the subsurface).¹⁰ For comparison with subsurface B, however, we also consider subsurface P in this work. The adsorption of water (H₂O) and ammonia (NH₃) on Si(001) is primarily governed by surface charge polarization, thereby making it ideal for exploring dopant-modified surface properties. In addition, H₂O and NH₃ surface reactions technologically play an important role in oxide (SiO₂) and nitride (Si₃N₄) film formation, respectively.

2. Computational Details

All geometric structures and total energies are calculated using the planewave-basis pseudopotential method within the generalized gradient approximation (GGA)¹¹ to density functional theory (DFT), as implemented in the Vienna Ab initio Simulation Package (VASP).^{12–14} We use Vanderbilt-type ultrasoft pseudopotentials^{15,16} and planewave basis sets with a cutoff energy of 300 eV. The Si(001) surfaces are modeled using a five-atomic-layer slab separated from its vertical periodic images by a six-atomic-layer vacuum space. We check the convergence with respect to the vacuum space by increasing its thickness up to 16 atomic layers, showing that changes in adsorption energy are less than 0.02 eV (which is within the tolerance of chemical accuracy, 1 kcal/mol = 0.04 eV). The bottom-layer Si atoms are fixed at the bulk position, and their dangling bonds

* To whom correspondence should be addressed. E-mail: gshwang@che.utexas.edu. Phone: 512-471-4847. Fax: 512-471-7060.

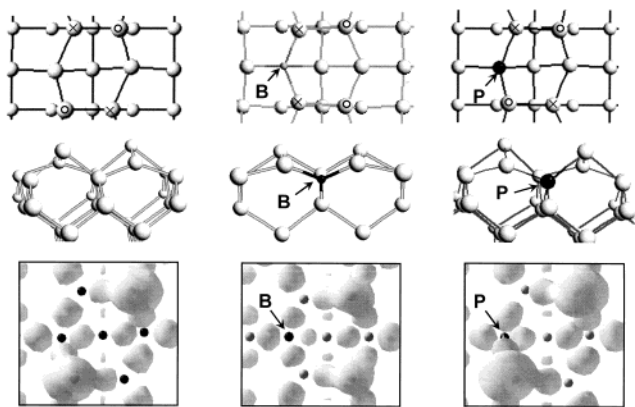


Figure 1. Top (top) and side (middle) view, together with ELF = 0.8 isosurface maps (bottom), of Si(001) surfaces: (a) clean, (b) B-modified, and (c) P-modified.

are passivated by H atoms. The topmost four layers and adsorbates are fully relaxed until all residual forces become smaller than 0.01 eV/Å. We use (4×4) and (4×5) surface cells for the clean/P-modified and B-modified Si(001) surfaces, respectively. The unit cells are large enough to eliminate a lateral interaction between an adsorbate and its periodic images. We used a $(2 \times 2 \times 1)$ mesh of k points in the scheme of Monkhorst–Pack for the surface Brillouin zone sampling and the tetrahedron smearing method with Blöchl corrections.¹⁷

The electron localization function (ELF)¹⁸ is employed to analyze the nature of bonding and nonbonding interactions. ELF represents the electron pair localization in terms of the conditional probability of finding an electron in the neighborhood of another electron with the same spin. By definition, ELF ranges from 0 to 1, with perfect localization corresponding to 1. Typically, relatively large values of $\text{ELF} \geq 0.5$ represent the regions of bonding and nonbonding localized electrons, whereas smaller values of < 0.5 suggest regions of delocalized electrons. Thus, ELF isosurface maps provide a clear picture for the positions of the bonding and nonbonding regions of localized electron pairs.

Charge density difference maps are used to examine the redistribution of surface charges upon molecular H_2O and NH_3 adsorption. We also use the GAMESS electronic structure program¹⁹ to calculate changes in the charge state of surface atoms and adsorbates in the adsorption systems. The Hay–Wadt effective core potential (ECP) with its associated basis sets²⁰ and the hybrid exchange correlation functional (B3LYP)²¹ are used.

3. Results and Discussion

3.1. Surface Properties. **3.1.1. Clean Si(001) Surface.** It is well-known that surface atoms of Si(001) are dimerized to reduce the surface energy. At low temperatures (< 200 K), Si–Si dimers appear to remain alternately buckled along a dimer row, with antiphase correlation between dimer rows, leading to the well-ordered $c(4 \times 2)$ structure (Figure 1a). The antiferromagnetic phase is widely accepted as the ground state of Si(001),²² although a controversy still remains.

For the $c(4 \times 2)$ state, our DFT–GGA calculation yields a bond length of 2.33 Å and a buckling angle of 18.6°, in good agreement with previous DFT calculations.^{23,24} The dimer buckling brings about partial charge transfer from the buckled-down atom to the buckled-up atom,^{25,26} as demonstrated by ELF in Figure 1a (bottom). (Nonbonding localized electrons are shown on top of buckled-up Si atoms. Here, the value for all

ELF isosurfaces is set at 0.8.) Buckling-induced charge transfer results in two groups of chemically inequivalent surface atoms; that is, buckled-down atoms are electron-poor (electrophilic), and buckled-up atoms are electron-rich (nucleophilic). Our cluster calculation shows that these up and down atoms are charged at -0.16 e and $+0.16$ e, respectively.

3.1.2. B-Modified Si(001) Surface. B incorporation into the subsurface significantly alters the local surface structure, because of its small atomic radius. The distances of ~ 2.0 Å between B and the nearest surface Si atoms are much shorter than corresponding Si–Si bond lengths of ~ 2.4 Å on the clean surface. As a consequence, two B-connected Si atoms are placed at the buckled-down position; that is, these two adjacent dimers are oriented in the same direction (Figure 1b). Their bond length and buckling angle are 2.33 Å and 15.5°, respectively. Because of the symmetry change, the B-modified surface is modeled using a (4×5) surface cell.

Our study also predicts that subsurface B alters substantially the charge polarization of B-connected dimers. (Note that B's electronegativity is 2.04, which is larger than the value of 1.90 for Si.) It appears that approximately one electron is transferred from B-connected dimers to subsurface boron (which has three valence electrons). As a result, both up and down atoms of these B-connected dimers become electron-poor (electrophilic), although electron depletion of up atoms is minimal. On the local surface, at least, none of Si atoms is electron-rich (nucleophilic). The B effect is likely to be well localized. (The charge states of second-nearest dimers are barely affected by the boron incorporation.) The charge transfer from the surface to the subsurface boron can be demonstrated by the smaller size of ELF isosurfaces on B-connected dimers (Figure 1b) relative to the clean surface (Figure 1a).

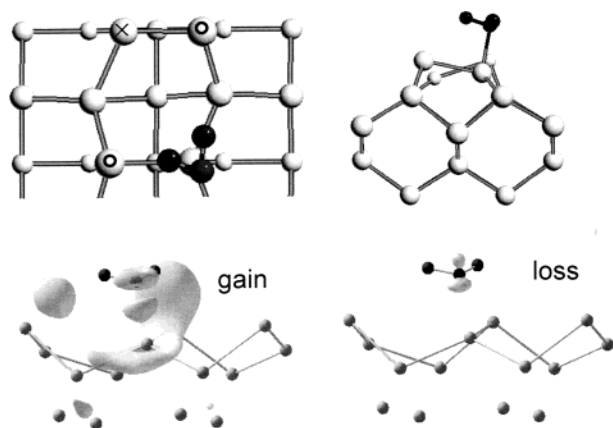
3.1.3. P-Modified Si(001) Surface. Because P's atomic radius of ~ 1.0 Å is close to the value of ~ 1.1 Å for Si, P insertion into the subsurface insignificantly changes the atomic structure of P-connected dimers. The lengths and buckling angles of the next neighboring dimers are calculated to be 2.34–2.38 Å and 19.3–20.5°, respectively, close to values for the clean surface (Figure 1c).

There is partial charge transfer to the surface from subsurface P (which has five valence electrons). According to our cluster calculation, approximately 0.14 e is transferred mainly to the buckled-up Si atom directly connected to P. The transferred electron would fill the antibond π^* -state, which may in turn weaken the Si–Si bonding interaction in the dimer (as evidenced by the increased bond length by 0.05 Å). This result suggests that subsurface P results in an increase in surface energy, consistent with experimental observations that P prefers to reside on the surface, rather than in the subsurface.

For P-connected dimers, a small amount of charge (less than one-tenth of an electron) is additionally transferred from the buckled-down atom to the -up atom. (As shown in Figure 1c, there is no significant change in ELF isosurfaces when P is placed in the subsurface.) The P-modified and clean surfaces exhibit a similar behavior in surface charge polarization, indicating that subsurface P has a much smaller effect on the surface reactivity than subsurface B.

3.2. H₂O Adsorption. **3.2.1. Clean Si(001) Surface.** The lowest-energy adsorption structure and charge density changes upon H_2O adsorption on the clean surface are displayed in Figure 2a. The resulting adsorption properties are summarized in Table 1. As predicted by previous first-principles studies,^{27,28} H_2O preferably adsorbs on an electrophilic buckled-down atom (via electrostatic interaction between the negatively charged O

A. Molecular adsorption



B. Dissociative adsorption

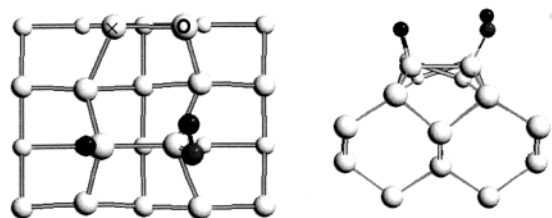


Figure 2. H₂O adsorption structures on clean Si(001) and charge density differences (i.e., gain and loss, as indicated) upon H₂O adsorption. The buckled-up and -down Si atoms are marked by a circle (○) and a cross (×), respectively. The dark small and large balls represent H and O atoms, respectively.

TABLE 1: Adsorption Properties of Water on the Clean Si(001) Surface

	E_{ad}^a (eV)	$d_{\text{Si-Si}}^b$ (Å)	α^c (deg)	$d_{\text{Si-O}}^d$ (Å)	$d_{\text{O-H}}^e$ (Å)
surf		2.33	18.6		
mol	0.73	2.40	11.7	1.99	1.01 (1.03)
dis	2.55	2.43	0.9	1.67	0.99

^a E_{ad} = adsorption energy. ^b $d_{\text{Si-Si}}$ = dimer bond length. ^c α = dimer buckling angle. ^d $d_{\text{Si-O}}$ = distance between the O atom of water and the nearest Si surface atom. ^e $d_{\text{O-H}}$ = O–H bond length of water.

of H₂O and the electrophilic buckled-down Si atom). When H₂O is placed on top of a buckled-up atom (followed by geometry optimization), the host dimer is flipped so that the up atom becomes buckled down. This result suggests that the up-atom site is unfavorable for molecular H₂O adsorption. For the molecular adsorption state, one O–H bond of H₂O points to the buckled-up atom in the host dimer, and the other O–H bond points to the up atom of an adjacent dimer. This is due primarily to the electrostatic interaction between positive H atoms and negative (nucleophilic) buckled-up Si atoms.

From our DFT-GGA calculations, the adsorption energy is predicted to be 0.73 eV (with no adsorption barrier), in good agreement with the value of 0.5–0.6 eV from previous DFT calculations.^{27,28} The relatively small adsorption energy suggests that the weak dative bonding of Si–OH₂ is mainly responsible for molecular H₂O adsorption on clean Si(001). Upon H₂O adsorption, while the atomic structure of H₂O remains nearly unchanged, the host dimer configuration changes noticeably. (The bond length increases from 2.33 to 2.40 Å, and the buckling angle decreases from 18.6° to 11.7°.) Given that a normal Si–Si σ -bond length is about 2.40 Å, it is likely that

H₂O adsorption leads to the π -bonding disruption of the host dimer. There is no significant change in the configuration of neighboring dimers. Our cluster calculation shows approximately one-quarter of an electron is transferred from adsorbed H₂O to Si surface and subsurface layers, in turn stabilizing H₂O adsorption by reducing the repulsive interaction between Si dangling orbitals and H₂O lone electron pairs.²⁹ As shown in Figure 2a, the buckled-up atoms of the host dimer and one adjacent dimer (to which an O–H bond of adsorbed H₂O points) become more negatively charged.

Molecularly adsorbed H₂O may dissociate to OH and H via either the intradimer or interdimer channel. Estimated barriers for the intradimer and interdimer dissociations are 0.24 and 0.25 eV, respectively, in agreement with the value of 0.15 eV as predicted by previous DFT calculations²⁸ (for the intradimer dissociation). The small barriers imply that the H₂O dissociation may take place readily, even at moderated temperatures, with exothermicities of 1.8 and 1.5 eV for the intradimer and interdimer reactions, respectively. Therefore, the overall exothermicity for dissociative H₂O adsorption on clean Si(001) is predicted to be around 2.2–2.5 eV, in good agreement with 2.13–2.67 eV of previous DFT calculations.^{27,28} Because the intradimer state is more energetically stable than the interdimer state, it can be expected that the former will prevail at low-coverage dissociative adsorption at equilibrium (although both states can easily be accessible with virtually the same small barrier).

3.2.2. B-Modified Si(001) Surface. Figure 3a shows the lowest-energy configuration of molecularly adsorbed H₂O on the B-modified surface, together with electron density changes upon H₂O adsorption. The resulting adsorption properties are summarized in Table 2. H₂O adsorption on the B-modified surface shows distinctly different features from the clean surface, as summarized below, from B-induced surface charge redistribution.

1. Both buckled-up and -down atoms are stable for molecular H₂O adsorption.

2. Upon H₂O adsorption at the up atom site, the host dimer is stretched to 2.37 Å, and its buckling angle is reduced to 8.2°. The bond length of the other B-connected dimer also increases to 2.40 Å (indicating π -bonding disruption), but with stronger buckling.

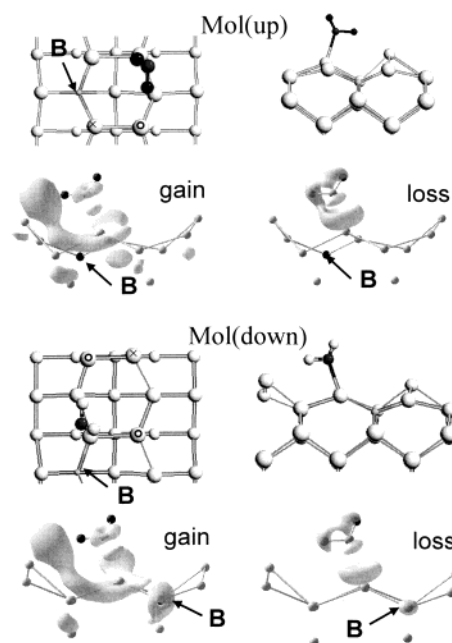
3. Upon H₂O adsorption at the down atom site, the host dimer is nearly symmetrized, and the other B-connected dimer is more strongly buckled. These two dimers are stretched only slightly (~2.35 Å), suggesting that their π -bonds are still preserved.

4. When H₂O adsorbs on the up site, an OH bond is directed toward the buckled-up atom of the other B-connected dimer (Figure 3a, mol(up)). The H···Si distance is 2.38 Å, which is quite short. However, OH does not directly point to the down site of the host dimer.

5. When H₂O adsorbs on the down site, one OH bond prefers to point to the buckled-up atom of another neighboring dimer (which is not connected to B) (Figure 3a, mol(down)), rather than the down atom of the B-connected dimer. In this case, OH does not directly point to the up atom of the host dimer either, implying that the up atom is insignificantly charged.

Given that molecular H₂O adsorption is mainly determined by surface charge polarization, the unusual adsorption behavior is apparently attributed to the charge state change of surface Si atoms. As mentioned earlier, unlike the clean surface, both up and down atoms of B-connected dimers are positively charged; at least, the up atoms are no longer significantly nucleophilic. Thus, both up and down sites can be favorable for nucleophilic–

A. Molecular adsorption



B. Dissociative adsorption

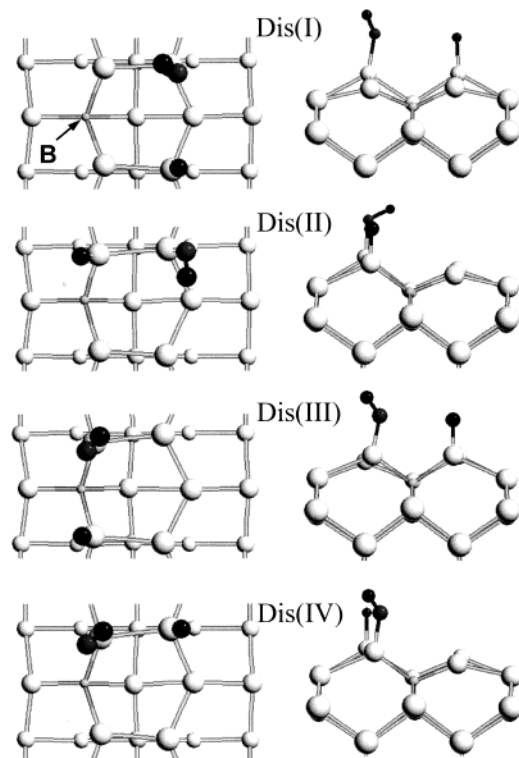


Figure 3. H₂O adsorption structures on B-modified Si(001) and charge density differences (i.e., gain and loss, as indicated) upon H₂O adsorption. The position of subsurface B is indicated. The buckled-up and -down Si atoms are marked by a circle (○) and a cross (×), respectively.

electrophilic H₂O adsorption. Considering their larger positive charge, buckled-down sites may be kinetically more favorable, though.

When H₂O adsorbs at the down site, a fair amount of charge is transferred to the up atom of the non-B-connected neighboring dimer. Thus, the up atom becomes more electron-rich, nucleophilic. This can explain why positively charged H is prefer-

TABLE 2: Adsorption Properties of Water on the B-Modified Si(001) Surface

	E_{ad}^a (eV)	d_{Si-Si}^b (Å)	α^c (deg)	d_{Si-O}^d (Å)	d_{O-H}^e (Å)
surf		2.33	15.5		
mol(up)	0.78	2.37	8.2	1.93	1.00
mol(down)	0.87	2.35	2.0	2.09	1.00
dis(I)	2.49	2.38	14.8	1.65	0.99
dis(II)	2.23	2.45	5.1	1.67	0.98
dis(III)	2.06	2.4	6.1	1.65	0.99
dis(IV)	2.34	2.43	3.1	1.67	0.98

^a E_{ad} = adsorption energy. ^b d_{Si-Si} = dimer bond length. ^c α = dimer buckling angle. ^d d_{Si-O} = distance between the O atom of water and the nearest Si surface atom. ^e d_{O-H} = O–H bond length of water.

ably directed toward the up Si atom. The formation of weak Si...H–O ionic bonding may stabilize further the H₂O adsorption. The H₂O adsorption energy is estimated to be 0.87 eV, as expected, 0.14 eV greater than the value of 0.73 eV on the clean surface. There is no significant charge transfer from the down to the up site in the nearly symmetrized host dimer. H₂O adsorption at the up site results in charge transfer (approximately one-quarter of an electron) to the up atom of the other B-connected dimer. The adsorption energy of 0.78 eV is comparable to 0.73 eV on the clean surface.

For dissociative H₂O adsorption, we consider four different states (Figure 3b). The overall exothermicity ranges from 2.06 to 2.46 eV. The most stable state appears to be dis(I), in which both H and OH fragments stay at the up sites of two B-connected dimers. From our DFT-GGA calculations, the interdimer dissociation barrier is estimated to be ~0.27 eV, comparable to the value of ~0.24–25 eV on the clean surface. Note that the positively charged H of molecularly adsorbed H₂O on a B-connected dimer strongly interacts with the negatively charged up Si of a neighboring dimer, rather than the positively charged up or down Si of the host dimer. This suggests that the H₂O dissociation on the B-modified surface may follow predominantly the interdimer mechanism, unlike on the clean surface.

Our calculation results suggest that subsurface incorporated B atoms would significantly alter (i) the configuration and charge polarization of two B-connected dimers as well as (ii) the (molecular and dissociative) adsorption structures of H₂O. While no direct evidence is available at present, measurements with scanning tunneling microscopes will serve for the validation of our conclusions. On the other hand, the barriers for H₂O molecular adsorption, dissociation, and associative desorption are likely to be insignificantly affected by the single B incorporation. Thus, we suspect it would be hard to detect directly the difference in chemical reactivity toward H₂O adsorption between the clean and B-modified surfaces by simply measuring the H₂O adsorption and desorption rates. Here, we only consider single B incorporation, but B atoms may also remain clustered at high doping levels. In this case, the H₂O adsorption and desorption behaviors may also change.

3.2.3. P-Modified Si(001) Surface. Figure 4a shows the configuration of adsorbed H₂O on the P-modified surface, together with charge density differences upon H₂O adsorption. The resulting adsorption properties are summarized in Table 3.

Like the clean surface, only the down sites are stable for H₂O adsorption. For the P-connected dimers, two groups of down sites exist: One is directly connected to P [mol(I)], and the other is not [mol(II)]. It turns out that the adsorption energies at these sites are comparable, ~0.80–0.86 eV. One O–H bond of the adsorbed H₂O points to the buckled-up atom of the host dimer, and the other points to the buckled-up atom of an adjacent dimer. The host dimer is substantially stretched to about 2.4 Å, with a buckling angle of 10.8–12.6°.

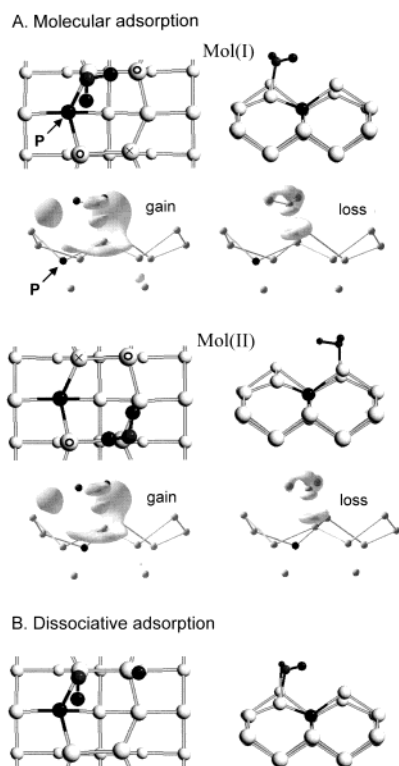


Figure 4. H₂O adsorption structures on P-modified Si(001) and charge density differences (i.e., gain and loss, as indicated) upon H₂O adsorption. The position of subsurface P is indicated. The buckled-up and -down Si atoms are marked by a circle (○) and a cross (×), respectively.

TABLE 3: Adsorption Properties of Water on the P-Modified Si(001) Surface

	E_{ad}^a (eV)	d_{Si-Si}^b (Å)	α^c (deg)	d_{Si-O}^d (Å)	d_{O-H}^e (Å)
surf		2.35(2.39)	19.3		
mol(I)	0.86	2.39	12.6	1.98	1.01
mol(II)	0.80	2.42	10.8	2.01	1.01
dis	2.73	2.41	0.7	1.66	1.00

^a E_{ad} = adsorption energy. ^b d_{Si-Si} = dimer bond length. ^c α = dimer buckling angle. ^d d_{Si-O} = distance between the O atom of water and the nearest Si surface atom. ^e d_{O-H} = O–H bond length of water.

H₂O dissociation into OH and H follows predominantly the intradimer mechanism (Figure 4b). The overall exothermicity is estimated to be 2.73 eV, about 0.2 eV greater than on the clean surface. The H₂O adsorption behavior is similar overall to that on the clean surface.

3.3. NH₃ Adsorption. **3.3.1. Clean Si(001) Surface.** Figure 5a shows the configuration of adsorbed NH₃ and charge density changes (upon NH₃ adsorption) on the clean surface. The resulting adsorption properties are summarized in Table 4. On the clean surface, like H₂O, molecular NH₃ adsorption is initiated by the electrostatic interaction between the negatively charged N of NH₃ and an electrophilic down site, with no barrier. By donating the N lone pair to the down Si atom of the host dimer, NH₃ is datively bonded to the surface.

The structure of adsorbed NH₃ changes unnoticeably, while the configuration of the host dimer is significantly altered. (The bond length and buckling angle change to 2.42 Å and 11.0°, respectively, indicating the π -bonding disruption of the host dimer.) It appears that approximately one-half of an electron is transferred from the adsorbed NH₃ molecule to both surface and subsurface Si atoms. Notice that the amount of transferred charge is twice as large as the H₂O adsorption. The buckled-up

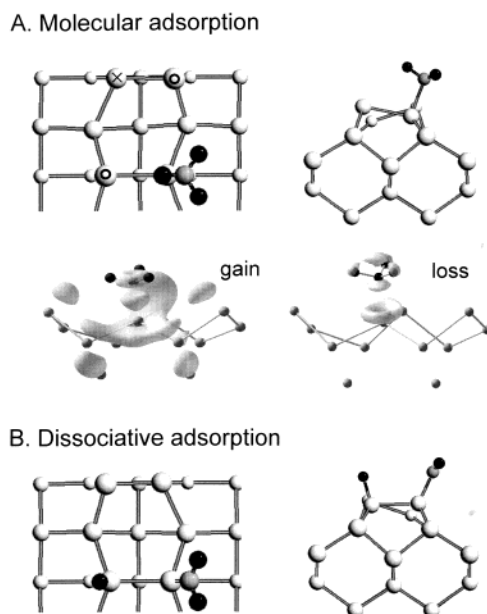


Figure 5. NH₃ adsorption structures on clean Si(001) and charge density differences (i.e., gain and loss, as indicated) upon NH₃ adsorption. The buckled-up and -down Si atoms are marked by a circle (○) and a cross (×), respectively. The dark small and large balls represent H and O atoms, respectively.

TABLE 4: Adsorption Properties of Ammonia on the Clean Si(001) Surface

	E_{ad}^a (eV)	d_{Si-Si}^b (Å)	α^c (deg)	d_{Si-N}^d (Å)	d_{N-H}^e (Å)
mol	1.44	2.42	11.3	1.99	1.03
dis	2.07	2.40	2.2	1.675	1.01

^a E_{ad} = adsorption energy. ^b d_{Si-Si} = dimer bond length. ^c α = dimer buckling angle. ^d d_{Si-N} = distance between the N atom of ammonia and the nearest Si surface atom. ^e d_{N-H} = N–H bond length of ammonia.

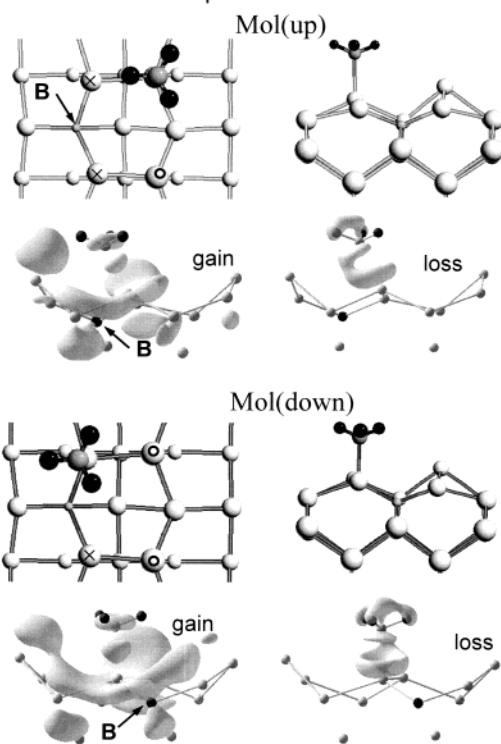
atoms of the host and next-neighboring dimers become more negatively charged because of such an electron gain, as illustrated in Figure 5a.

The molecularly adsorbed NH₃ undergoes exothermic dissociation to NH₂ and H mostly by the intradimer mechanism (Figure 5b). The dissociation reaction is activated, with a barrier of about 0.6 eV.³⁰ Overall, the exothermicity of dissociative NH₃ adsorption is estimated to be ~2.07 eV, in excellent agreement with experimental values (~2.04 eV)³¹ and previous DFT-GGA results (~2.0 eV).³⁰

3.3.2. B-Modified Si(001) Surface. Figure 6a shows the configuration of adsorbed NH₃ on the B-modified surface. The adsorption properties are summarized in Table 5. Our results show that the up and down sites both are favorable for molecular NH₃ adsorption; the corresponding adsorption energies are estimated to be 1.46 and 1.62 eV, respectively. Changes in the structural and electronic properties of B-connected dimers (upon NH₃ adsorption) are similar to those upon H₂O adsorption. Compared to the clean surface, more charge appears to be transferred to adjacent buckled-up atoms (particularly at the mol-(down) state), which may result in a stronger Si(up)···H–N electrostatic interaction. Indeed, the adsorption energy of 1.62 eV at the mol(down) state is about 0.2 eV greater than on the clean surface.

Here, we consider two different dissociation states, interdimer [dis(I)] and intradimer [dis(II)], as shown in Figure 6b. Their adsorption energies are comparable, ~2.35 eV, suggesting that both intradimer and interdimer states are thermodynamically

A. Molecular adsorption



B. Dissociative adsorption

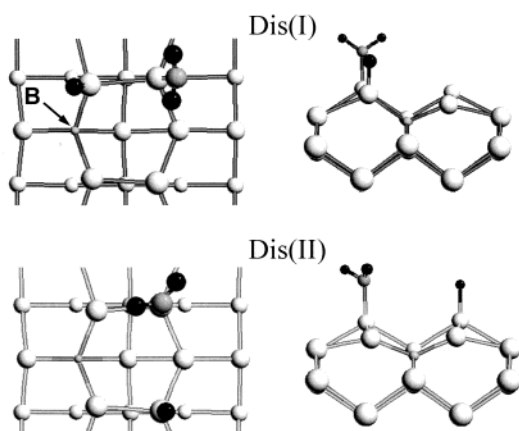


Figure 6. NH_3 adsorption structures on B-modified Si(001) and charge density differences (i.e., gain and loss, as indicated) upon NH_3 adsorption. The position of subsurface B is indicated. The buckled-up and -down Si atoms are marked by a circle (○) and a cross (×), respectively.

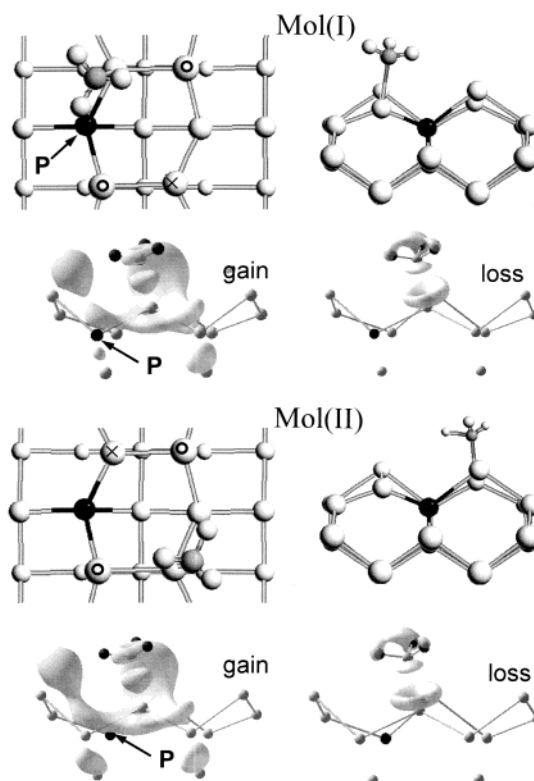
TABLE 5: Adsorption Properties of Ammonia on the B-Modified Si(001) Surface

	E_{ad}^a (eV)	$d_{\text{Si-Si}}^b$ (Å)	α^c (deg)	$d_{\text{Si-N}}^d$ (Å)	$d_{\text{N-H}}^e$ (Å)
mol(up)	1.46	2.35	11.4	1.96	0.98 (1.05, 1.09)
mol(down)	1.62	2.37	0.7	1.98	1.05
dis(I)	2.35	2.38	11.7	1.74	1.02
dis(II)	2.34	2.38	12.1	1.74	1.00

^a E_{ad} = adsorption energy. ^b $d_{\text{Si-Si}}$ = dimer bond length. ^c α = dimer buckling angle. ^d $d_{\text{Si-N}}$ = distance between the N atom of ammonia and the nearest Si surface atom. ^e $d_{\text{N-H}}$ = N-H bond length of ammonia.

favorable. On the clean surface, the interdimer state is less favorable than the intradimer state, because the former leaves two dangling orbitals on the surface.

A. Molecular adsorption



B. Dissociative adsorption

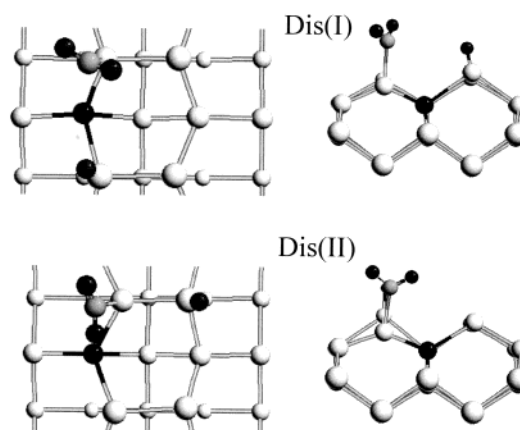


Figure 7. NH_3 adsorption structures on P-modified Si(001) and charge density differences (i.e., gain and loss, as indicated) upon NH_3 adsorption. The position of subsurface P is indicated. The buckled-up and -down Si atoms are marked by a circle (○) and a cross (×), respectively.

TABLE 6: Adsorption Properties of Ammonia on the P-Modified Si(001) Surface

	E_{ad}^a (eV)	$d_{\text{Si-Si}}^b$ (Å)	α^c (deg)	$d_{\text{Si-N}}^d$ (Å)	$d_{\text{N-H}}^e$ (Å)
mol(I)	1.36	2.40	12.0	1.98	1.03
mol(II)	1.45	2.44	11.8	1.98	1.03
dis(I)	1.94	2.41	6.2	1.70	1.01
dis(II)	2.36	2.43	1.4	1.72	1.02

^a E_{ad} = adsorption energy. ^b $d_{\text{Si-Si}}$ = dimer bond length. ^c α = dimer buckling angle. ^d $d_{\text{Si-N}}$ = distance between the N atom of ammonia and the nearest Si surface atom. ^e $d_{\text{N-H}}$ = N-H bond length of ammonia.

3.3.3. P-Modified Si(001) Surface. Figure 7a shows two different configurations of adsorbed NH_3 on the P-modified surface. The adsorption properties are summarized in Table 6

and are very close to those on the clean surface. NH_3 adsorbs only on the down sites. The adsorption energies are calculated to be 1.36 and 1.45 eV, respectively, at two inequivalent down sites [mol(I) and mol(II)]. The host dimer bond length increases by ~ 0.6 Å, and its buckling angle decreases by $\sim 8^\circ$. NH_3 dissociation follows mainly the intradimer mechanism, with overall exothermicity of 2.36 eV (somewhat larger than the value of 2.07 eV on the clean surface).

4. Summary

On the basis of first-principles quantum mechanics calculations, we present changes in the structural and chemical properties of Si(001) when B or P dopant atoms are incorporated into the subsurface. Subsurface B alters significantly the buckling structure and charge polarization of the two B-connected dimers. Because of the small B atomic radius, two B-connected Si surface atoms are placed at the buckled-down position; that is, these dimers are oriented in the same direction. In addition, our calculations predict substantial charge transfer from the local surface to the subsurface B, thereby making both up and down atoms electron-poor (electrophilic). On the other hand, subsurface P results in insignificant changes in the atomic and electronic structures of P-connected dimers. Only a small amount of charge is transferred from the subsurface P to the surface.

We also present H_2O and NH_3 adsorption properties on the B- and P-modified surfaces. Because of a significant change in charge polarization on the B-modified surface, the adsorption properties are distinctly different from those of the clean surface, including the following: (i) both the buckled-up and -down atoms are stable sites for molecular H_2O and NH_3 adsorption; (ii) upon H_2O adsorption at the down atom site, the host dimer is almost symmetrized, and the other B-connected dimer gets more strongly buckled, but the B-connected dimers π -bonds are not completely disrupted; and (iii) upon H_2O adsorption at the up atom site, the bond length of the other B-connected dimer increases with stronger buckling, showing its π -bonding disruption. We attribute the difference in adsorption properties to charge redistribution on the B-modified local surface. The subsurface B effect is likely to appear stronger in the adsorption of H_2O than NH_3 . On the other hand, incorporation of P into the subsurface turns out to barely affect the H_2O and NH_3 adsorption properties. Here, we only consider single B and P atoms. However, a large fraction of dopants could remain clustered at very high doping levels,^{32,33} and further investigation on the effect of dopant clusters is warranted.

Our study demonstrates that dopant impurities can be used for atomic-scale manipulation of surface chemical properties.

Such detailed understanding will assist in (i) improving present device fabrication technologies and (ii) finding a new and reliable way to construct self-assembled organic structures on a semiconductor surface for future molecular devices.

Acknowledgment. The authors acknowledge the Welch Foundation (Grant F-1535) for their financial support of this work.

References and Notes

- (1) Yates, J. T. *Science* **1998**, 279, 335.
- (2) Hamers, R. J. *Nature* **2001**, 412, 489.
- (3) Bent, S. F. *J. Phys. Chem. B* **2002**, 106, 2830.
- (4) Copel, M.; Reuter, M. C.; Kaxiras, E.; Tromp, R. M. *Phys. Rev. Lett.* **1989**, 63, 632.
- (5) Doris, B.; Fretwell, J.; Erskine, J. L.; Banerjee, S. K. *Appl. Phys. Lett.* **1997**, 70, 2819.
- (6) Hamers, R. J.; Wang, Y.; Shan Appl. Surf. Sci. **1996**, 107, 25.
- (7) Gong, B.; Brown, D. E.; Kang, J. H.; Jo, S. K.; Sun, Y. M.; Ekerdt, J. G. *Phys. Rev. B* **1999**, 59, 15225.
- (8) Wang, Y.; Hwang, G. S. *Surf. Sci.* **2003**, 547, L882.
- (9) Tersoff, J. *Phys. Rev. Lett.* **1995**, 74, 5080.
- (10) Ramamoorthy, M.; Briggs, E. L.; Bernholc, J. *Phys. Rev. Lett.* **1998**, 81, 1642.
- (11) Perdew, J.; Chevary, J.; Vosko, S.; Jackson, K.; Pederson, M.; Singh, D.; Fiolhais, C. *Phys. Rev. B* **1992**, 46, 6671.
- (12) Kresse, G.; Hafner, J. *Phys. Rev. B* **1993**, 47, 558.
- (13) Kresse, G.; Furthmüller, J. *Comput. Mater. Sci.* **1996**, 6, 15.
- (14) Kresse, G.; Furthmüller, J. *Phys. Rev. B* **1996**, 54, 11169.
- (15) Vanderbilt, D. *Phys. Rev. B* **1990**, 41, 7892.
- (16) Kresse, G.; Hafner, J. *J. Phys.: Condens. Matter* **1994**, 6, 8245.
- (17) Blöchl, P. E.; Jepsen, O.; Andersen, O. K. *Phys. Rev. B* **1993**, 49, 16223.
- (18) Becke, A. D.; Edgecombe, K. E. *J. Chem. Phys.* **1990**, 92, 5397.
- (19) Schmidt, M. W.; Baldrige, K. K.; Boatz, J. A.; Elbert, S. T.; Gordon, M. S.; Jensen, J. H.; Koseki, S.; Matsunaga, N.; Nguyen, K. A.; Su, S. J.; Windus, T. L.; Dupuis, M.; Montgomery, J. A. *J. Comput. Chem.* **1993**, 14, 1347.
- (20) Wadt, W. R.; Hay, P. J. *J. Chem. Phys.* **1985**, 82, 284.
- (21) Becke, A. D. *J. Chem. Phys.* **1993**, 98, 5648.
- (22) Healy, S. B.; Filippi, C.; Kratzer, P.; Penev, E.; Scheffler, M. *Phys. Rev. Lett.* **2001**, 87, 16105.
- (23) Gay, S. C. A.; Srivastava, G. P. *Phys. Rev. B* **1999**, 60, 1488.
- (24) Hwang, G. S. *Surf. Sci.* **2000**, 465, L789.
- (25) Chadi, D. J. *Phys. Rev. Lett.* **1979**, 43, 43.
- (26) Landemark, E.; Karlsson, C. J.; Chao, Y. C.; Uhrberg, R. I. G. *Phys. Rev. Lett.* **1992**, 69, 1588.
- (27) Konečný, R.; Doren, D. J. *J. Chem. Phys.* **1997**, 106, 2426.
- (28) Cho, J. H.; Kim, K. S.; Lee, S. H.; Kang, M. H. *Phys. Rev. B* **2000**, 61, 4503.
- (29) Eyal, F.; Radeke, M. R.; Reynolds, G.; Carter, E. A. *J. Phys. Chem. B* **1997**, 101, 8658.
- (30) Lee, S. H.; Kang, M. H. *Phys. Rev. B* **1998**, 58, 4903.
- (31) Dresser, M. J.; Taylor, P. A.; Wallace, R. M.; Choyke, W. J.; Yates, J. T., Jr. *Surf. Sci.* **1989**, 218, 75.
- (32) Wang, Y.; Hammers, R.; Kaxiras, E. *Phys. Rev. Lett.* **1995**, 74, 403.
- (33) Ramamoorthy, R.; Briggs, E. L.; Bernholc, J. *Phys. Rev. B* **1999**, 59, 4813.